Eur. Phys. J. D **35**, 249–255 (2005)
DOI: 10.1140/epjd/e2005-00082-0

THE EUROPEAN PHYSICAL JOURNAL D

Probing the isomer, fluorination and bond effects in C_3H_6, cyclo-C_3H_6 and C_3F_6 molecules using electron impact

C. Makochekanwa[1,2,a], H. Kato[2], M. Hoshino[2], H. Cho[3], M. Kimura[1], O. Sueoka[4], and H. Tanaka[2]

[1] Graduate School of Sciences, Kyushu University, Fukuoka 812-8581, Japan
[2] Department of Physics, Sophia University, Tokyo 102-8554, Japan
[3] Physics Department, Chungnam National University, Daejeon 305-764, South Korea
[4] Faculty of Engineering, Yamaguchi University, Ube 755-8611, Japan

Received 31 March 2005/ Received in final form 17 April 2005
Published online 7 June 2005 –

Abstract. We have carried out experimental and theoretical studies on electron scattering from the C_3H_6 isomers and C_3F_6 molecules and we report on total, differential as well as theoretical integral elastic cross-sections for these molecules. Vibrational excitation functions are also presented for the typical vibrational peaks in C_3H_6 and cyclo-C_3H_6 for the angle of 90°, impact energy range of 1–16 eV and loss energies of 0.12 eV and 0.13 eV, respectively. In the cross-sections, clear differences in peak positions and magnitudes between the C_3H_6 isomers can be viewed as the isomer effect. The same is observed between C_3H_6 and C_3F_6 in a clear manifestation of the fluorination effect. The resemblance of the π^* shape resonance in the cross-sections, observed at about 2.2 eV for C_3H_6 and 3.5 eV for C_3F_6, to those in C_2H_4 and C_2F_4 clearly points to the effect of the double bond in the molecular structures for these molecules. Theoretical analysis is performed to provide rationales for the scattering dynamics.

PACS. 34.80.Bm Elastic scattering of electrons by atoms and molecules – 34.80.Gs Molecular excitation and ionization by electron impact

1 Introduction

Hydrocarbons play an important role for plasma diagnostics as impurities in the Tokamak fusion divertor, as seed gases for production of radicals and ions in low-temperature plasma processing, and many other fields [1]. On the other hand, fluorine-substituted hydrocarbons, the so-called perfluorocarbons (PFCs), are not the less important also as they play significant roles as reactive agents in plasma-assisted fabrication processes [2]. Based on these and other reasons, both classes of molecules have received some research attention from both theorists and experimentalists over the past few decades. Needless to point out that a comparative study of these PFCs with pure hydrocarbons helps in the establishment of the role of microscopic molecular properties of the target in the electron scattering processes.

The two stable isomers of the C_3H_6 molecules; propene (H_3C–CH=CH_2) and cyclo-propane [*cyclic*(H_2C–CH_2–CH_2)] are studied for the isomer effect owing to their characteristic differences in physical and chemical properties, whilst the hexafluoropropene [F_3C–CH=CF_2] molecule offers an opportunity for studying the effects of fluorine atom substitution on the electronic structure and spectra of propene. Note that a study of the fluorination effect between cyclo-C_3H_6 and cyclo-C_3F_6 could also have been interesting, but the latter is not commercially available. Some similarities observed in the cross-sections for C_3H_6 and C_3F_6 can be traced back to the C_2H_4 and C_2F_4, in a clear reflection of the double bond effect in these molecules.

Though some studies have been performed on these molecules, they have centered mainly on either one of these molecules, as for example propene (C_3H_6) [3–7], cyclo-C_3H_6 [8–12], and C_3F_6 [13–18]. To our knowledge, there exist however, some few attempts that studied the isomer effect in these molecules by electron impact total cross-sections [19,20], ionization cross-sections [21,22] and differential cross-sections [23]. There also exist some vacuum ultraviolet (VUV) studies of the isomer effect in the optical oscillator strengths for these isomers [24]. Another study worth mentioning is that by Floeder et al. [25] who, though not directly studying this effect, studied total cross-sections, including those for these two molecules, in their systematic study of the scattering cross-sections for the alkane and alkene molecular families.

We have undertaken the present work to study the isomer, fluorination and bond effects in experimental electron impact total cross-sections (TCSs), differential cross-sections (DCSs) and theoretical integral elastic

[a] e-mail: c-makoch@sophia.ac.jp

cross-sections (ECSs), and in the vibrational excitation functions for these molecules. We examine the similarities and differences observed in the cross-sections between the molecules for the isomer, fluorination and bond effects, and also provide some rationale based on the collision dynamics for electron impact with molecules.

2 Experimental and theoretical approaches

2.1 Total cross-sections (TCS)

A retarding-potential time-of-flight (RP-TOF) apparatus [26,27] was used for the TCS experiments. The electron beam source was a $\sim$80 μCi ^{22}Na radioactive isotope, whereby the beam is produced as secondary electrons coming out of the positron moderator surfaces. The electron beam energy width was about 1 eV. The energy resolution, however, is determined by the RP-TOF and is below 0.3 eV below impact energies of 4 eV [28]. The TCSs for all three molecules have been confirmed to be pressure-independent in the present energy range by carrying out independent test experiments. This is an important check parameter for experiments carried out using a collision cell in the transmission RP-TOF set-up.

The experimental uncertainties involved in these measurements are due to errors in statistics, collision cell effective length determination, gas density and the forward scattering correction. The estimates for the sum of the first three terms amounted a maximum 4.0%, 3.6% and 4.0% for C_3H_6, cyclo-C_3H_6 and C_3F_6 electron TCSs, respectively. The details pertaining to the forward scattering effect and the method for the correction was described elsewhere [26,29].The electron DCSs being jointly presented in this paper were used for correction of the TCSs for each molecules, after using the molecular phase shift approach [30] in order to extrapolate the DCSs to the experimentally inaccessible scattering angles, i.e. down to 0° and up to 180°. The main part of the correction process involves calculation of the transmission function, which itself is a function of the magnetic field used (4.5 G in these experiments), impact energy, the position coordinate parallel to the flight path, the radial position coordinate, collision cell aperture diameter and the collision cell effective length [29]. The forward scattering correction rates show some typical variation across the current range of impact energies. For example, this correction for C_3F_6 electron TCSs ranged between 2.6% and 4.2% below 10 eV, an average 4.4% at 10–30 eV, and decreased from 3.8% to 1.4% with increasing energy from 35 eV to 1 000 eV.

2.2 Elastic and vibrational differential cross-sections

The apparatus used in the present DCS measurements is the same as used in our previous studies [31]. The overall energy-resolution was 35–40 meV, and the angular resolution was $\pm$ 1.5°. Hence, the present DCSs are considered to be the sum of the elastic process and the rotational excitation and de-excitation processes, and some vibrational levels. But, in C_3H_6, the energy-loss peak for the constituent stretching vibrational modes are separated from the elastic one with the present energy resolution. By using the energy excitation mode, the incident energy dependence is also observed for the vibrational excitation. Absolute cross-sections for the elastic scattering cross-sections were obtained by the relative flow technique [32] using helium as the reference gas. The electron energy scale was calibrated with respect to the 19.367 eV resonance for He. Experimental errors in the DCSs were estimated to be 15–20%.

2.3 Theoretical model

The theoretical approach employed is the continuum multiple-scattering (CMS) method [33].The CMS method divides the molecular configuration space into three regions. Region I: the atomic region surrounding each atomic sphere, region II: the interstitial, and region III: the outer region surrounding the molecule. The atomic sphere is chosen to enclose each atom with an origin at each nucleus. Each sphere attaches to every other. Region III is chosen to enclose all of the atomic spheres. In general, the potential for the scattered electron in each region of space is approximated by the spherical potential in regions I and III and by a constant in region II, which should be determined by averaging the potentials of regions I and III. From the SCF calculation that includes static and exchange terms for the composite $(n+1)$ electron system, then the spherical part of the potential is extracted around each nucleus as the effective potential for the incident electron. The static interaction was obtained by using the Hartree-Fock method, while the exchange interaction was determined by the Slater Xα method [34]. The potential in region III decays rapidly enough at large r. The potential may be approximated by the sum of the monopole terms. For a nonpolar molecule, the polarization potential α/r^{-4} may be appropriate, while the dipole potential d/r^2 may be used for a polar molecule. Hence, the scattering part of the method is regarded as the static-exchange-dipole (polarization for non-polar molecules) potential model within the fixed-nuclei approximation [33,35,36]. The Schrödinger equation in each region is solved numerically under separate boundary conditions, and by matching the wave functions one can determine the total scattering wave functions, the scattering matrix and hence, the total cross-sections by a conventional procedure [36].

3 Results and discussions

3.1 Comparison between C_3H_6 and cyclo-C_3H_6: the isomer effect

Figure 1 shows the present TCS and ECS results for these molecules. A comment is warranted here on the comparison between the current results and the previous results

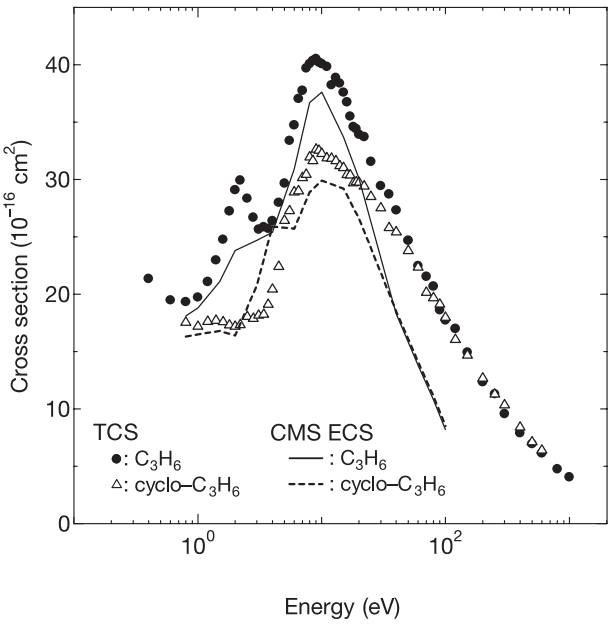

Fig. 1. C_3H_6 and cyclo-C_3H_6 electron impact TCSs and CMS ECSs. Thresholds for ionization are at 9.73 eV for C_3H_6, and 9.86 eV for cyclo-C_3H_6.

available in literature, though this will not be allowed to overshadow the discussions of the effects, which are the theme of this report. For C_3H_6, except for the region <0.8 eV where the current data rises, our TCSs agree well in structure with the only available previous results in references [19,20,25]. However, for both molecules, some magnitude differences are observed at the peaks, for example our result is less than the largest of the three (Szmytkowski et al. [20]) by more than 12% at 2.2 and 9.5 eV, while greater than the lowest of the three (Floeder et al. [25]) data by about 15% at 9.5 eV. For cyclo-C_3H_6, though the current result agrees so well both qualitatively and quantitatively with the Floeder et al. over all the energy range of overlap, only good qualitative agreement is observed with the other two data sets. Detailed comparative studies of the present TCSs with these results by other groups will be carried out in separate papers soon to follow on these molecules.

3.1.1 TCSs

Figure 1 shows the current TCS results for these molecules. The comparative features observed in these data are summarized as follows. C_3H_6 TCSs are greater than cyclo-C_3H_6 TCSs at all energies below 60 eV. At the energy range below 1 eV, C_3H_6 TCSs begin to rise while cyclo-C_3H_6 TCSs are still on the plateau. The C_3H_6 TCSs show a lower energy peak at about 2.2 eV before the larger and broader one at about 9 eV. Beyond this main peak, these TCSs decrease rather monotonously, and become nearly equal to the cyclo-C_3H_6 TCSs beyond 50 eV. In contrast, cyclo-C_3H_6 TCSs are basically flat below 3 eV and show a change of slope in the curve at about 6 eV before the main peak also centered at about 9 eV. The onset of the rising trend below 1 eV in C_3H_6 TCSs, but not in cyclo-C_3H_6 TCSs, should be associated with the enhanced scattering at these lower energies in C_3H_6 due to the presence of the small electric dipole moment (0.366 D) for C_3H_6, whereas cyclo-C_3H_6 molecules are non-polar. The relatively larger polarizability for C_3H_6 (6.26×10^{-30} m^3 for C_3H_6, 5.66×10^{-30} m^3 for cyclo-C_3H_6) should also result in enhanced lower energy forward scattering in C_3H_6 compared to cyclo-C_3H_6. The peak at about 2.2 eV in C_3H_6 is attributable to the shape resonance due to vibrational excitation of the molecules, as can be clearly seen in the vibrational excitation functions of the bending vibrational mode v_3, with a peak at around 2 eV, for these molecules in Figure 3. This proceeds via formation of the transient ion due to the incident electron being trapped temporarily into valance orbitals with the C=C antibonding character, i.e. the lowest unoccupied molecular orbital (LUMO). In the elastic scattering channel, elastic scattering via resonances is in general smeared out by the direct elastic component. However, these resonances can in most cases be clearly revealed in vibrational excitation functions for experiments done whilst sweeping impact energies across the resonance region, i.e. as in Figure 3. This peak has also been associated with the π^* shape resonance in the theoretical studies by Winstead et al. [23]. A resonance arising from the stretching vibrational excitation (v_3 mode) motion of the C–C (ring) has been reported at about 6 eV for cyclo-C_3H_6 [8,37–39]. Notice however, that though Curik et al. [39] observe this feature at 6.4 eV in their vibrationally inelastic calculations, references [37,38], as well as our result in Figure 3, show this feature in the experimental functions for vibrational excitation at about 5.5 eV. However, except for the slight change of slope observed at about 6 eV, this feature is almost invisible in the cyclo-C_3H_6 TCS curve of Figure 1, possibly because of the small magnitude of the absolute cross-sections for this vibrational resonance compared to the TCSs which are about 29×10^{-16} cm^2 in this region. As for the common broad peak centered at about 9 eV for both molecules, the cyclo-C_3H_6 peak has been attributed to the shape resonance in symmetry of the D_{3h}, which is symmetric with respect to the CCC (σ_h) plane but antisymmeteric in each of the three σ_v planes [23]. This peak in C_3H_6 should be attributable to the A_1' symmetry type of shape resonance that we have observed to be characteristic of hydrocarbons resulting in peaks in this region, although contributions from other several inelastic scattering processes should also be significant (see our result in Figure 3, and also Refs. [3,40]). The near equal TCSs above 50 eV, is rather unexpected though because the molecularly larger C_3H_6 TCSs should be greater than those for cyclo-C_3H_6. (Note that as reported already by Nishimura and Tawara [19], the ring structure of cyclo-C_3H_6 makes it to be more compact than the linear C_3H_6, resulting in a larger spatial electron distribution for the latter than the former. This larger electron spatial distribution for C_3H_6 would then be expected to result in larger scattering TCSs than cyclo-C_3H_6.)

Also shown in Figure 1 are the current theoretical ECSs. For each molecule, these ECS results reproduce the structures observed in the TCSs well. Except that the ECSs for C_3H_6 and cyclo-C_3H_6 nearly equal each other around 4 eV, magnitude differences can clearly be seen in these ECSs in the regions around the resonance peaks, i.e. below 30 eV. At the higher energy side of the main peak, i.e. above 35 eV, the ECSs for both molecules nearly become equal within experimental error. However, the CMS ECS result for cyclo-C_3H_6 is unexpectedly greater than the TCS at the energy range 2–5 eV, and shows a rather sharp shoulder at about 4 eV, i.e. in a way failing to reproduce the TCS. Otherwise, differences between the ECSs and the TCSs just emphasize the importance of the inelastic channels. Above the thresholds for ionization, i.e. 9.73 eV for C_3H_6, and 9.86 eV for cyclo-C_3H_6, the ionization channel should be the dominant inelastic channel contributing to the TCS. See the ionization cross-sections for these molecules in references [21,22]. Below these ionization thresholds, contributions from vibrational (see Fig. 3) and electronic excitation as well as electron attachment processes should combine to make up this difference.

3.1.2 DCSs

The present results, shown in Figure 2, are found to agree well both qualitatively and quantitatively at overlapping energies with the only available two theoretical results [37,39] on the two isomers, and one experimental result [41] on cyclo-C_3H_6. The detailed comparative study of the present results with these results by other groups is intentionally left out to the next papers under preparation on these molecules. The reason is simply that this report is exclusively focusing on this isomer effect. The lowest energy of 2.0 eV shows results with the most drastic difference between these two isomer molecules, C_3H_6 and cyclo-C_3H_6, with the DCSs for the two nearly equaling each other at 20°, the former being higher in the range 20°–100°, and vice versa above 100°. The rising DCSs trend towards 0° is only expected for C_3H_6, and not for cyclo-C_3H_6, as a result of enhanced forward scattering due to the presence of the dipole moment and larger polarizability in the former, as pointed out above. However, the fact that cyclo-C_3H_6 DCSs are also rising at this energy is either puzzling, or simply indicating that this is already too high an energy to observe pure dipole scattering effects. Besides, that the larger DCSs for the former rise to produce the peak-like structure above 60°, is consistent with the peak observed in both the ECSs and TCSs at around 2.2 eV. This DCS angular distribution is characteristic of the *d*-wave scattering. Whereas the C_3H_6 DCSs show two shallow minima, a forward-angle one centered at about 50° and a higher-angle one at about 110°, cyclo-C_3H_6 DCSs show only one clear minimum, i.e. at the same forward-angle of 50° as in C_3H_6, C_3H_6 shows another higher angle minimum at about 110°. However, the forward-angle minimum is clearly much deeper in the former than the latter. These minima however, slowly become deeper with increasing impact energy for C_3H_6,

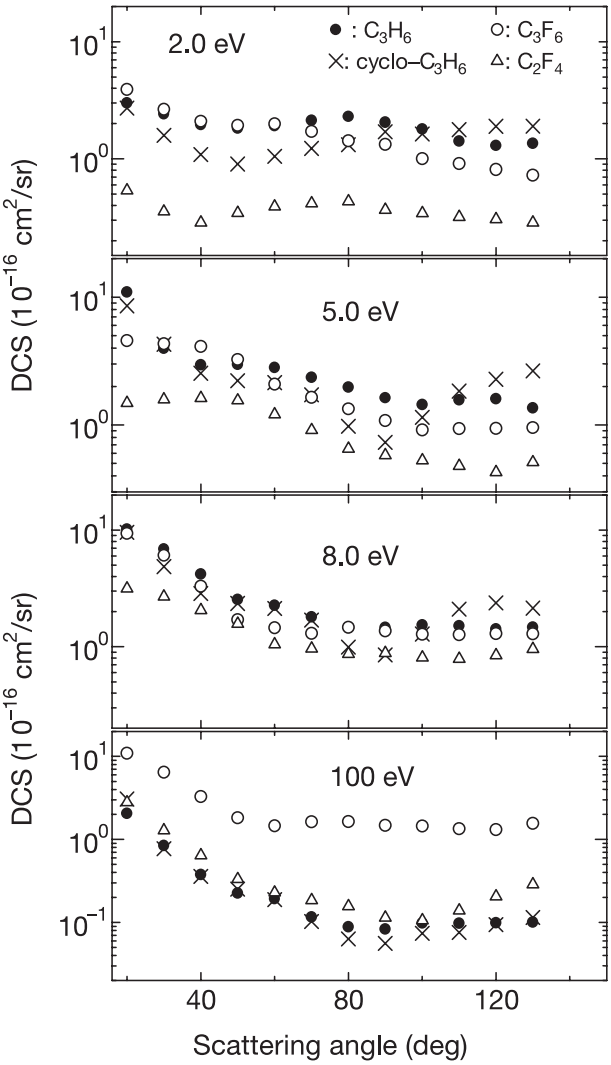

Fig. 2. C_3H_6, cyclo-C_3H_6 and C_3F_6 electron impact DCSs, together with those of C_2F_4 [43].

and are seen to be each drifting towards lower angles. At 5.0 eV, the forward-angle one is already at the edge for C_3H_6, i.e. at about 35°, in the limit of the minimum measured angle of 20°, and completely disappears at 8.0 eV, while that for cyclo-C_3H_6 is at the same angle, but shallower. The higher-angle peak in C_3H_6 now sits at about 100° at 5.0 eV. It's also clear that cyclo-C_3H_6 DCSs have also developed a higher-angle minimum that is deeper and appears at about 90°. At this energy, except for the angle of 30° where the DCSs for these two molecules nearly equal each other, C_3H_6 DCSs are larger than cyclo-C_3H_6 DCSs below 110°, and vice versa above this angle. At 8.0 eV and 100 eV, the DCSs for these two molecules nearly equal each other below 60°, pointing to some insensitivity of the electron scattering to the molecular geometry at these energies and angles. However, some slight differences can still be seen even at these energies at angles above 60°.

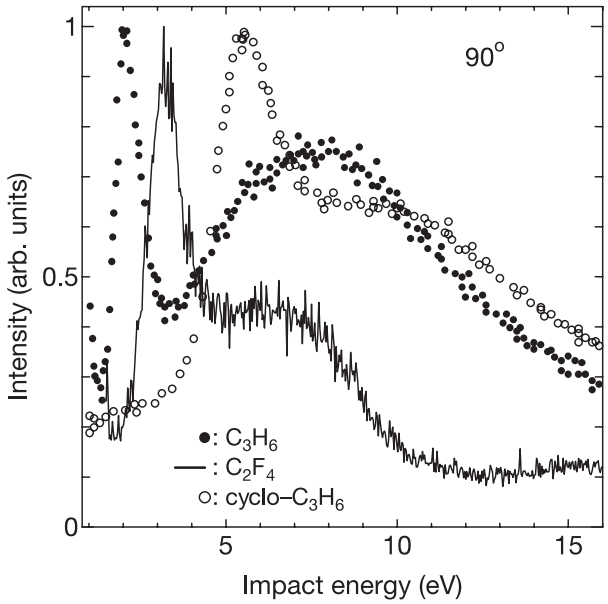

Fig. 3. Vibrational excitation functions for C_3H_6 (bending v_3 mode) and cyclo-C_3H_6 (bending v_2 mode) at 90° and energy losses of 0.12 eV and 0.13 eV, respectively. C_2F_4 data from reference [43] are also shown for 90° and the energy loss of 0.16 eV.

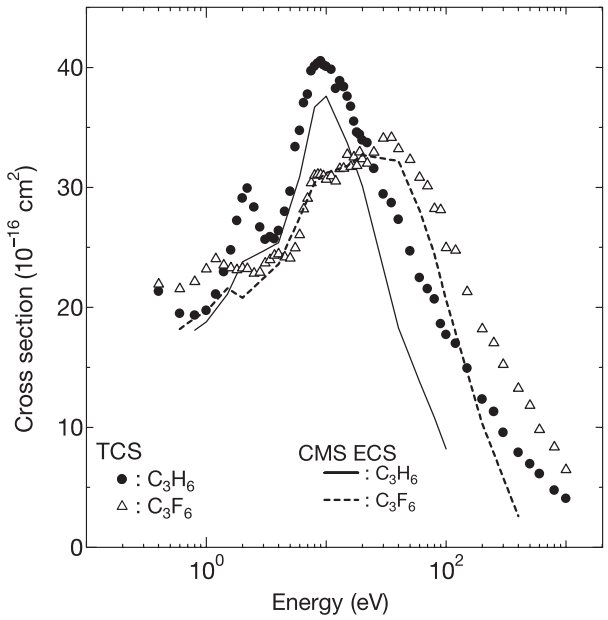

Fig. 4. C_3H_6 and C_3F_6 electron impact TCSs and CMS ECSs. The threshold for ionization is at 10.60 eV for C_3F_6. See caption for Figure 1 for that for C_3H_6.

3.2 Comparison between C_3H_6 and C_3F_6: the fluorination effect

Figure 4 shows the present TCS and ECS results for these molecules. Once again, a comment is warranted here on the comparison between the current C_3F_6 results and the previous data available in literature [17,18,42]. The current TCSs show general agreement in the energy dependence with the results by these two groups above 50 eV. However, even in this energy region, the current TCSs are smaller than these two, with the difference in magnitudes between the current data and the Szmytkowski et al. [17,18] data increasing from about 15% at 50 eV to about 24% at 370 eV. The Jiang et al. [42] data continues to rise below this energy of 50 eV. Szmytkowski et al. report resonances at energies 3.2 eV, 9 eV and the broader one extending from 20 to 70 eV (NB. they did not report on this third one maybe because it just fell on the edge of their differently published 30–370 eV and 0.5–30 eV results, with no combined data plot from them). This clearly differs from the current results especially with regards to the other structures we observe at 1.2 eV and the 14–22 eV region. Besides, there seems to be some slight energy position difference in the commonly observed second resonance as we observe it at about 3.6 eV (versus their 3.2 eV). Once again, because we are only exclusively focusing on this fluorination effect, we will not get into details of carrying out the comparative analysis of the current results with these literature results by other groups, and leave this out to the coming papers.

3.2.1 TCSs

It is interesting to note the way the fluorination effect is reflected in the TCSs shown in Figure 4. These observations are summarized as follows.

(i) C_3F_6 TCSs are greater than C_3H_6 TCSs below 1.4 eV, although the two nearly equal each other at the lowest applied energy of 0.4 eV.

(ii) C_3H_6 TCSs are greater than C_3F_6 TCSs in the range 1.5–25 eV.

(iii) C_3F_6 TCSs show a lower energy resonance peak at about 1.2 eV. Vibrational excitation studies are awaited for the clarification of the nature and origin of this peak which, however, should be resonant in nature.

(iv) The C_3F_6 TCSs show another peak at 3.6 eV while C_3H_6 TCSs show one at 2.2 eV. We note that this peak in C_3F_6 TCSs, just as in C_3H_6 TCSs too, should be attributable to the π^* shape resonance that we have systematically observed to be a feature arising due to the double in a molecular structure resulting in the incident electron being trapped temporarily into the valance orbitals with the C=C antibonding character. See for example our earlier studies on C_2F_4 [43] and C_3H_4 [44], to name a few. The C_3F_6 peak however, should also have contributions from some resonances arising from the temporary capture of the electron by the target molecule with the creation of an intermediate parent anion leading to the formation of negative ions [45,46].

(v) Whereas C_3H_6 TCSs show the single main peak at about 9 eV, C_3F_6 TCSs show multiple peaks, i.e. at about 8.5 eV, the unclearly resolved 14–22 eV region and the broad one at about 30 eV. That is, the C_3F_6 TCS peak is significantly broader than that of the C_3H_6 TCSs. The features at about 8.5 eV and in the unclearly resolved region of 14–22 eV should also attributable to the production of the numerous negative ions that have been observed at around these regions [45,46].

(vi) Beyond their respective peaks, both TCSs decrease monotonically, albeit with the C_3F_6 TCSs overtaking the C_3H_6 TCSs to become significantly greater in magnitude above 25 eV. This is rather expected as C_3F_6 are larger in molecular size than C_3H_6 molecules.

The theoretical ECS results are also shown in Figure 4. It is worth noting that these ECSs show the same relative magnitude behavior between these two molecules just as observed in the just discussed TCSs, i.e. C_3H_6 ECSs relatively greater than C_3F_6 ECSs below about 15 eV, before the reverse becomes true above this energy. It worth noting too though that the broadening observed in the C_3F_6 TCSs is also reproduced by the ECS result. This aspect of peak broadening of TCSs has also been observed as a persistent aspect of the fluorination effect in other sets of pure hydrocarbon versus PFC studies we have carried out before. See for example reference [29]. On the relative magnitudes between these ECSs and TCSs, contributions from the ionization channel, i.e. with thresholds at 9.73 eV for C_3H_6 and 10.6 eV for 9.73 eV C_3F_6, and other inelastic channels should increasingly become significant above the main resonance peaks for these TCSs. This is evidenced by the increasing differences between their respective TCSs and ECSs above 10 eV and 50 eV for C_3H_6 and C_3F_6, respectively. See the ionization cross-sections for these two molecules in references [16,21].

3.2.2 DCSs

The C_3H_6 and C_3F_6 results for these molecules are shown in Figure 2. We are not aware of any previous work that dealt with elastic DCSs for scattering from the C_3F_6 molecules. At the lowest energy of 2.0 eV, both DCSs show some rising trend towards 0°, as expected for these polar molecules, as pointed out earlier. However, in a manifestation of the fluorination effect, C_3H_6 DCSs are seen to be greater than the C_3F_6 counterpart in the range above 70°. The DCSs show two shallow minima, a forward-angle one centered at about 50° and a higher-angle one at about 110°. These minima however, slowly become deeper with increasing impact energy, and are seen to be each drifting towards lower angles. At 5.0 eV, the forward-angle one is almost gone for C_3F_6 while almost at the edge for C_3H_6, in the limit of the minimum measured angle of 20°, and completely disappears at 8.0 eV. At this energy, the higher-angle one now sits at about 90° for both molecules. At 100 eV, C_3F_6 DCSs become greater than C_3H_6, i.e. being an average ten times greater. This should be an effect due to the larger molecular size in case of the C_3F_6 molecules.

3.3 Comparison between C_3H_6 and C_3F_6 with C_2H_4 and C_2F_4: the bond effect

As partially pointed out above, the low energy shape resonance observed in both TCSs and ECSs at about 2.2 eV in C_3H_6 and 3.6 eV in C_3F_6, but not in cyclo-C_3H_6 can be traced back to the C=C double bonding in the molecular structures for these molecules. This peak has been observed in the TCSs and ECSs for simpler double-bond containing molecules: i.e. at about 1.9 eV in C_2H_4 TCSs [47] and ECSs [30]; and at about 2.8 eV in C_2F_4 TCSs [48] and ECSs [43]. Figure 3 shows this resonance peak in the vibrational excitation functions for the present results, in comparison with those for C_2F_4. In both C_2H_4 and C_2F_4, this peak has been attributed to the $^2B_{2g}$ symmetry shape resonance which, in both cases, is a π^* type. The shift in the energy positions of this shape resonance peaks between the pure hydrocarbons and the perfluorocarbons (PFCs) has been discussed in the case of C_2H_4 and C_2F_4 and attributed to the non-planar structure of the $C_2F_4^-$ ion, of C_{2h} symmetry, and having pairs of F atoms attached to C atoms bent upwards and downwards relative to the C=C bond plane [48]. Since we observe a similar shift between the peak positions of this resonance for C_3H_6 and C_3F_6, we infer that the same phenomenon could be responsible for this too. Note also that the C=C bond length in C_3H_6 is 1.341 Å compared to 1.329 Å for C_3F_6 [49]. In general, as the effective range of an interaction decreases, the height of the potential barrier trapping the incoming electron tends to increase.

4 Conclusion

In this paper we report on experimental and theoretical studies probing the isomer, fluorination and bond effects in electron impact TCSs, DCSs and ECSs for C_3H_6, cyclo-C_3H_6 and C_3F_6 molecules. Vibrational excitation functions have also been studied, for C_3H_6 and cyclo-C_3H_6, and aided in elucidating the nature of the resonances observed at 2.2 eV (C_3H_6), 3.5 eV (cyclo-C_3H_6) and around 9 eV. We have observed clear differences in peak positions and magnitudes between the C_3H_6 isomers which we regard as *the isomer effect*. Similar features were observed between C_3H_6 and C_3F_6, which we regard as due to the substitution of the H atom by the F atom; *the fluorination effect*. The effect of the double bond in the molecular structures was identified for these molecules following the resemblance of the π^* shape resonance observed in C_3H_6 and C_3F_6 to those in C_2H_4 and C_2F_4; *the bond effect*.

The work was supported in part by a Grant-in-Aid, the Ministry of Education, Science, Technology, Sport and Culture, Japan, the Japan Society for the Promotion of Science (JSPS), the Japan Atomic Energy Research Institute and a cooperative grant from National Institute for Fusion Science (MK). This work was also partially supported by the CUP program between Japan and South Korea. CM and MK are also grateful to the JSPS for financial support under the grant number P04064, and also to Yamaguchi University as CM did part of this work whilst he was a Ph.D. student there.

References

1. W.L. Morgan, Adv. At. Mol. Opt. Phys. **43**, 79 (2000)
2. Y. Hatano, Adv. At. Mol. Opt. Phys. **43**, 231 (2002)
3. C.R. Bowman, W.D. Miller, J. Chem. Phys. **42**, 681 (1965)

4. K.E. Johnson, D.B. Johnston, S. Lipsky, J. Chem. Phys. **70**, 3844 (1979)
5. L.-P. Wang, R. Hinkelman, W.T. Tysoe, J. Electron Relat. Phenom. **56**, 341 (1991)
6. M.P. Banjavcic, T.A. Daniels, K.T. Leung, Chem. Phys. **155**, 309 (1991)
7. E. Engeln, J. Reuss, Chem. Phys. **156**, 215 (1991)
8. M. Allan, J. Am. Chem. Soc. **115**, 6418 (1993)
9. K.H. Sze, C.E. Brion, J. Electron Relat. Phenom. **57**, 117 (1991)
10. H.H. Brongersma, L.J. Oosterhoff, Chem. Phys. Lett. **3**, 437 (1969)
11. H. Basch, M.B. Robin, N.A. Kuebler, C. Baker, D.W. Turner, J. Chem. Phys. **51**, 52 (1969)
12. C. Fridh, J. Chem. Soc. Faraday Trans. **75**, 993 (1979)
13. S. Eden, P. Limao-Vieira, S.V. Hoffmann, N.J. Mason, Chem. Phys. Lett. **379**, 170 (2003)
14. C.A. Longfellow, L.A. Smoliar, Y.T. Lee, Y.R. Lee, C.Y. Yeh, S.M. Lin, Chem. Phys. Lett. **271**, 33 (1997)
15. G.K. Jarvis, K.J. Boyle, C.A. Mayhew, R.P. Tuckett, J. Phys. Chem. A **102**, 3230 (1998)
16. M. Bart, P.W. Harland, J.E. Hudson, C. Vallance, Phys. Chem. Chem. Phys. **3**, 800 (2001)
17. C. Szmytkowski, S. Kwitnewski, P. Mozejko, E. Ptasinska-Denga, Phys. Rev. A **66**, 014701 (2002)
18. C. Szmytkowski, P. Możejko, S. Kwitnewski, J. Phys. B **35**, 1267 (2002)
19. H. Nishimura, H. Tawara, J. Phys. B **24**, L363 (1991)
20. C. Szmytkowski, S. Kwitnewski, J. Phys. B **35**, 2613 (2002)
21. H. Nishimura, H. Tawara, J. Phys. B **27**, 2063 (1994)
22. H. Deutsch, K. Becker, R.K. Janev, M. Probst, T.D. Mark, J. Phys. B **33**, L865 (2000)
23. C. Winstead, Q. Sun, V. McKoy, J. Chem. Phys. **96**, 4246 (1992)
24. H. Koizumi, T. Yoshimi, K. Shinsaka, M. Ukai, M. Morita, Y. Hatano, A. Yagishita, K. Ito, J. Chem. Phys. **82**, 4856 (1985)
25. K. Floeder, D. Fromme, W. Raith, A. Schwab, G. Sinapius, J. Phys. B **18**, 3347 (1985)
26. O. Sueoka, S. Mori, J. Phys. B **19**, 4035 (1986)
27. A. Hamada, O. Sueoka, J. Phys. B **27**, 5055 (1994)
28. M. Kimura, C. Makochekanwa, O. Sueoka, J. Phys. B **37**, 1461 (2004)
29. O. Sueoka, C. Makochekanwa, H. Kawate, Nucl. Instr. Meth. B **192**, 206 (2002)
30. R. Panajotovic, M. Kitajima, H. Tanaka, M. Jelisavcic, J. Lower, L. Campbell, M.J. Brunger, S.J. Buckman, J. Phys. B **36**, 1615 (2003)
31. H. Tanaka, T. Ishikawa, M. Masai, T. Sagara, L. Boesten, M. Takekawa, Y. Itikawa, M. Kimura, Phys. Rev. A **57**, 1798 (1998)
32. S.K. Srivastava, A. Chutjian, S. Trajmar, J. Chem. Phys. **63**, 2659 (1975)
33. M. Kimura, H. Sato, Comments At. Mol. Phys. **26**, 333 (1991)
34. J.C. Slater, *Quantum Theory of Matter* (McGraw Hill, NY, 1968)
35. P.G. Burke, W.D. Robb, Adv. At. Mol. Phys. **11**, 143 (1975)
36. N.F. Lane, Rev. Mod. Phys. **52**, 29 (1980)
37. T. Beyer, B.M. Nestmann, B.K. Sarpal, S.D. Peyerimhoff, J. Phys. B **30**, 3431 (1997)
38. B.M. Nestmann, J. Phys. B **31**, 3929 (1998)
39. R. Curik, F.A. Gianturco, J. Phys. B **35**, 1235 (2002)
40. F.D. Dance, I.C. Walker, Proc. R. Soc. A **334**, 259 (1973)
41. M. Allan, in *Electron Collisions with Molecules, Clusters and Surfaces*, edited by H. Ehrhardt, L.A. Morgan (Plenum, New York, 1994)
42. Y. Jiang, J. Sun, L. Wan, Phys. Rev. A **62**, 062712 (2000)
43. R. Panajotovic, M. Jelisavcic, R. Kajita, T. Tanaka, M. Kitajima, H. Cho, H. Tanaka, S.J. Buckman, J. Chem. Phys. **121**, 4559 (2004)
44. C. Makochekanwa, H. Kawate, O. Sueoka, M. Kimura, M. Kitajima, M. Hoshino, H. Tanaka, Chem. Phys. Lett. **368**, 82 (2003)
45. P.W. Harland, J.C.J. Thynne, Int. J. Mass Spectrom. Ion Phys. **9**, 253 (1972)
46. C. Lifshitz, R. Grajower, Int. J. Mass Spectrom. Ion Phys. **10**, 25 (1972-3)
47. O. Sueoka, S. Mori, J. Phys. B **22**, 963 (1989)
48. C. Winstead, V. McKoy, J. Chem. Phys. **116**, 1380 (2002)
49. "Bond Legths and Angles in Gas-Phase Molecules" in *CRC Handbook of Chemistry and Physics*, edited by D.R. Lide, 81st edn. (CRC Press, NY, 2000-2001)